C. R. Mecanique 347 (2019) 191–206

Contents lists available at ScienceDirect

Comptes Rendus Mecanique

www.sciencedirect.com

Automated numerical simulation of the propagation of multiple cracks in a finite plane using the distributed dislocation method

Jiong Zhang [a], Zhan Qu [b], Weidong Liu [c], Liankun Wang [a,*]

[a] School of Civil Engineering and Architecture, Wuyi University, 22 Dongcheng Village, Jiangmen 529020, PR China
[b] School of Aeronautics, Northwestern Polytechnical University, 127 Youyi West Road, Xi'an 710072, PR China
[c] College of Energy and Electrical Engineering, Hohai University, No. 8 Fochengxi Road, Nanjing 211100, PR China

ARTICLE INFO

Article history:
Received 16 April 2018
Accepted 21 January 2019
Available online 11 February 2019

Keywords:
Distributed dislocation
Multiple cracks
Finite plane
Fatigue propagation

ABSTRACT

In this paper, an automated numerical simulation of the propagation of multiple cracks in a finite elastic plane by the distributed dislocation method is developed. Firstly, a solution to the problem of a two-dimensional finite elastic plane containing multiple straight cracks and kinked cracks is presented. A serial of distributed dislocations in an infinite plane are used to model all the cracks and the boundary of the finite plane. The mixed-mode stress intensity factors of all the cracks can be calculated by solving a system of singular integral equations with the Gauss–Chebyshev quadrature method. Based on the solution, the propagation of multiple cracks is modeled according to the maximum circumferential stress criterion and Paris' law. Several numerical examples are presented to show the accuracy and efficiency of this method for the simulation of multiple cracks in a 2D finite plane.

1. Introduction

Engineering materials or components usually contain cracks that were formed during manufacturing or localized damage. Those cracks may propagate until brittle fracture happens when the structures are subjected to cyclic loading. In this case, the analysis of the growth of fatigue cracks is very important to ensure the reliability of the structures. In linear fracture mechanics, the stress intensity factor of the crack is usually used to model crack propagation by successive crack growth. The propagation of multiple cracks is much more complicated than the propagation of a single crack because of interactions between the cracks. It requires the development and use of numerical methods to simulate the propagation of multiple cracks considering interactions between crack. Such an analysis requires an accurate knowledge of how the effects between each crack on the stress intensity factor and the fatigue propagation of the cracks.

The classic FEM is a typical numerical method to study the crack growth behavior for elastic materials [1–3]. However, the classic finite element method is not a good choice to perform the simulation of crack propagation for multiple cracks. Very good meshes are to be made near the crack tips to improve the accuracy of the stress intensity factors and remesh the structure after each crack extension. This needs a large computational cost, especially when the structure contains a large

* Corresponding author.
E-mail address: Fengzheng403@126.com (L. Wang).

https://doi.org/10.1016/j.crme.2019.01.004
1631-0721/

number of cracks. Besides, the computational efficiency is not high, since this method cannot transform the two-dimensional problem to a one-dimensional problem.

Recently, the XFEM was wildly used to simulate the crack growth behavior of two-dimensional materials [4–6]. This method is a convenient computational tool for modeling crack growth compared with traditional FEM, since it allows for the modeling of cracks to be independent of the finite element mesh. However, XFEM still cannot reduce the problem's dimensions and simplify the input requirements.

To solve the drawbacks mentioned above, we present a fully automatic simulation system of the growth of fatigue multiple cracks for a two-dimensional finite elastic plane based on the distributed dislocation method. The distributed dislocation method was firstly used to solve various kinds of crack problems in infinite mediums [7–13]. The principle of this method is to model the cracks by a serial of continuous dislocations in infinite media. Then the influence function of the dislocations is reduced to formulate a system of singular integral equations with Cauchy-type kernel. Moreover, the Gauss–Chebyshev quadrature method is usually used to deal with the singular integral equations. Some researchers also employed this method to study crack problems in a half plane [14–16]. This method was later extended to the study of cracking problems in a finite plane [17–19]. The boundaries of the plane were also modeled by the dislocations based on the boundary conditions. Besides, previous research also shows that the present method is very good at solving problems of multiple cracks and kinked cracks [15,16,19–21].

In this paper, firstly, we extend this method to solve the problem of a finite plane containing both multiple straight cracks and kinked cracks, which has never been reported. Then, based on the maximum circumferential stress criterion and Paris' law, fatigue propagation of multiple cracks was realized. However, we need to mention that the crack closure effects are not considered in this study.

This paper is structured as follows: Section 2 presents a detailed description of the distributed dislocation method to solve the problem of multiple cracks in a finite plane. Section 3 introduces the fatigue growth of multiple cracks in the frame of this paper. Section 4 shows some typical numerical examples of the presented method. Finally, some conclusions are given in Section 5.

2. Description of the presented numerical method

2.1. Decomposition of the problem of a finite plane containing multiple straight cracks and kinked cracks

A finite plane containing m_s straight cracks and m_k kinked cracks is subjected to an arbitrary applied load on the boundary, as shown in Fig. 1. All the cracks can have arbitrary lengths and inclination angles. The i-th kinked crack has p_i branches and the boundary of the plane contains m_b segments. This finite-plane problem, shown in Fig. 1, can be treated as a cut-out problem from an infinite plane [14]. The boundary also can be treated as a special kinked crack containing m_b branches. Now all the cracks can be modeled by continuous distributed dislocations in an infinite plane, as shown in Fig. 2. The original problem shown in Fig. 1 is essentially the same as that shown in Fig. 2, provided that, on the boundary, the stress matches the applied tractions and that the cracks lines are free of any traction:

- for cracks:

$$\begin{aligned} T(\hat{n}) = \sigma_{\hat{i}\hat{j}}(\hat{x}_i, 0) \cdot n_{\hat{j}}(\hat{x}_i, 0) &= \begin{bmatrix} \sigma_{\hat{x}\hat{x}}(\hat{x}_i, 0) & \sigma_{\hat{x}\hat{y}}(\hat{x}_i, 0) \\ \sigma_{\hat{x}\hat{y}}(\hat{x}_i, 0) & \sigma_{\hat{y}\hat{y}}(\hat{x}_i, 0) \end{bmatrix} \begin{bmatrix} n_{\hat{1}}(\hat{x}_i, 0) \\ n_{\hat{2}}(\hat{x}_i, 0) \end{bmatrix} \\ &= \begin{bmatrix} \sigma_{\hat{x}\hat{x}}(\hat{x}_i, 0) & \sigma_{\hat{x}\hat{y}}(\hat{x}_i, 0) \\ \sigma_{\hat{x}\hat{y}}(\hat{x}_i, 0) & \sigma_{\hat{y}\hat{y}}(\hat{x}_i, 0) \end{bmatrix} \begin{bmatrix} 0 \\ 1 \end{bmatrix} = \begin{bmatrix} 0 \\ 0 \end{bmatrix} \end{aligned} \tag{1}$$

- for the boundary:

$$T(\hat{n}) = \sigma_{\hat{i}\hat{j}}(\hat{x}_i, 0) \cdot n_{\hat{j}}(\hat{x}_i, 0) = \begin{bmatrix} \sigma^i_{\hat{x}\hat{x}}(\hat{x}_i, 0) & \sigma^i_{\hat{x}\hat{y}}(\hat{x}_i, 0) \\ \sigma^i_{\hat{x}\hat{y}}(\hat{x}_i, 0) & \sigma^i_{\hat{x}\hat{y}}(\hat{x}_i, 0) \end{bmatrix} \begin{bmatrix} 0 \\ 1 \end{bmatrix} = \begin{bmatrix} \sigma^0_{\hat{x}\hat{x}}(\hat{x}_i, 0) \\ \sigma^0_{\hat{x}\hat{y}}(\hat{x}_i, 0) \end{bmatrix} \tag{2}$$

In Eqs. (1) and (2), $\hat{x}_i$ is the local coordinate of a point on the i-th boundary branch as shown in Fig. 1, $T(\hat{n})$ is the applied traction outward unit vector normal to the i-th boundary, $n_{\hat{j}}(\hat{x}_i, 0)$ is the direction cosine of the outer normal victor of the i-th crack line, $\sigma_{\hat{i}\hat{j}}(\hat{x}_i, 0)$ are the stresses induced by the distributed dislocations in the local coordinates for the i-th boundary, and $\sigma^0_{\hat{i}}(\hat{x}_i, 0)$ are the applied stresses on the boundaries in the local coordinates for the i-th boundary. $\sigma^0_{\hat{1}}$, $\sigma^0_{\hat{2}}$ are the applied stress along and perpendicular to the crack line, respectively.

Equations (1) and (2) can be rewritten under the following form for simplicity:

- for cracks:

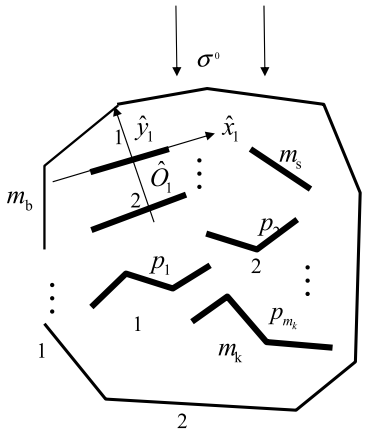

Fig. 1. A finite plane containing multiple straight and kinked cracks.

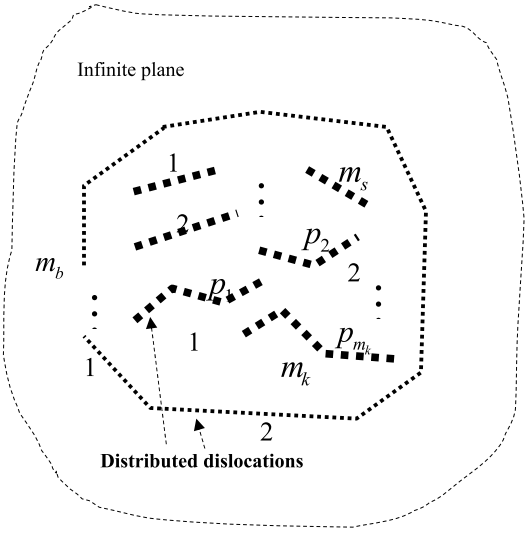

Fig. 2. A finite geometry as a cut-out from an infinite plane [14].

$$\begin{cases} \sigma^i_{\hat{x}\hat{y}}(\hat{x}_i, 0) = 0 \\ \sigma^i_{\hat{y}\hat{y}}(\hat{x}_i, 0) = 0 \end{cases} \tag{3}$$

- for the boundary:

$$\begin{cases} \sigma^i_{\hat{x}\hat{y}}(\hat{x}_i, 0) = \sigma^0_{\hat{1}}(\hat{x}_i, 0) \\ \sigma^i_{\hat{y}\hat{y}}(\hat{x}_i, 0) = \sigma^0_{\hat{2}}(\hat{x}_i, 0) \end{cases} \tag{4}$$

2.2. Dislocation influence function in an infinite elastic plane

Dislocation can be seen as a point source of strain or stress in this study. Then a crack can be modeled by a series of continuous dislocations along the crack line, if the unwanted tractions caused by the stresses of the dislocations along the crack line are canceled. So, in this part, we will firstly introduce the stress caused by an edge dislocation.

As shown in Fig. 3, an infinite plane contains an edge dislocation located at (ξ, η) with Burgers vector b_x, b_y. A point located at (x, y) in the plane has an induced stress field induced by the dislocation and can be expressed as follows [10],

$$\begin{bmatrix} \sigma_{xx}(x,y) \\ \sigma_{yy}(x,y) \\ \sigma_{xy}(x,y) \end{bmatrix} = \frac{2\mu}{\pi(\kappa+1)} \begin{bmatrix} G_{xxx}(x,y;\xi,\eta) & G_{yxx}(x,y;\xi,\eta) \\ G_{xyy}(x,y;\xi,\eta) & G_{yyy}(x,y;\xi,\eta) \\ G_{xxy}(x,y;\xi,\eta) & G_{yxy}(x,y;\xi,\eta) \end{bmatrix} \begin{bmatrix} b_x(\xi,\eta) \\ b_y(\xi,\eta) \end{bmatrix} \tag{5}$$

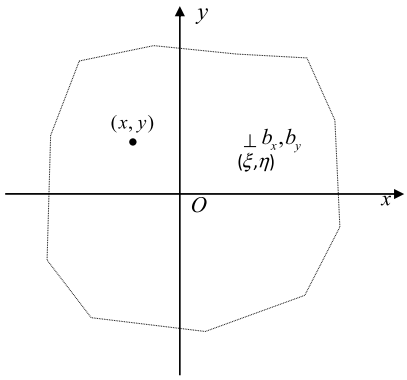

Fig. 3. Stresses induced due to the dislocation in an infinite plane.

where μ is the shear modulus of the plane, κ is Muskhelishvili's constant, $\kappa = (3-\nu)/(1+\nu)$ for plane stress, $\kappa = 3-4\nu$ for plane strain. ν is Poisson's ratio. Here the dislocation influence function G_{ijk} can be expressed in the global coordinates system by the following equations [10]:

$$\begin{cases} G_{xxx} = \left(-\dfrac{1}{r_1^2}\right)\left(1+\dfrac{2x_1^2}{r_1^2}\right); & G_{yxx} = \left(-\dfrac{x_1}{r_1^2}\right)\left(1-\dfrac{2x_1^2}{r_1^2}\right) \\ G_{xyy} = \left(-\dfrac{x_1}{r_1^2}\right)\left(1-\dfrac{2x_1^2}{r_1^2}\right); & G_{yyy} = \left(-\dfrac{1}{r_1^2}\right)\left(3-\dfrac{2x_1^2}{r_1^2}\right) \\ G_{xxy} = \left(-\dfrac{x_1}{r_1^2}\right)\left(1-\dfrac{2x_1^2}{r_1^2}\right); & G_{yxy} = \left(-\dfrac{1}{r_1^2}\right)\left(1-\dfrac{2x_1^2}{r_1^2}\right) \end{cases} \tag{6}$$

where $r^2 = x_1^2 + y_1^2$, $x_1 = x - \xi$, $y_1 = y - \eta$.

2.3. The governing integral equations

Based on previous research [10,15,19], we will deduce the governing integral equations for a finite plane containing multiple straight cracks and kinked cracks.

Consider a dislocation located at $(\hat{\xi}_j, 0)$ on the j-th crack branch. The induced stresses of the point $(\hat{x}_i, 0)$ on the i-th crack branch can be given, based on Eq. (4), by:

$$\begin{bmatrix} \sigma^{ij}_{\hat{x}\hat{x}}(\hat{x}_i,0) \\ \sigma^{ij}_{\hat{y}\hat{y}}(\hat{x}_i,0) \\ \sigma^{ij}_{\hat{x}\hat{y}}(\hat{x}_i,0) \end{bmatrix} = \frac{2\mu}{\pi(\kappa+1)} \begin{bmatrix} G^{ij}_{\hat{x}\hat{x}\hat{x}}(\hat{x}_i,0;\hat{\xi}_j,0) & G^{ij}_{\hat{y}\hat{x}\hat{x}}(\hat{x}_i,0;\hat{\xi}_j,0) \\ G^{ij}_{\hat{x}\hat{y}\hat{y}}(\hat{x}_i,0;\hat{\xi}_j,0) & G^{ij}_{\hat{y}\hat{y}\hat{y}}(\hat{x}_i,0;\hat{\xi}_j,0) \\ G^{ij}_{\hat{x}\hat{x}\hat{y}}(\hat{x}_i,0;\hat{\xi}_j,0) & G^{ij}_{\hat{y}\hat{x}\hat{y}}(\hat{x}_i,0;\hat{\xi}_j,0) \end{bmatrix} \begin{bmatrix} b_{\hat{x}}(\hat{\xi}_j,0) \\ b_{\hat{y}}(\hat{\xi}_j,0) \end{bmatrix} \tag{7}$$

It is more convenient to calculate the stress intensity factor if all the equations are expressed in the local coordinates of every crack branch. The corresponding transformation rules from global coordinates system to local coordinates can be summarized as follows [17]:

$$\begin{bmatrix} b^j_{\hat{x}}(\hat{\xi}_j,0) \\ b^j_{\hat{x}}(\hat{\xi}_j,0) \end{bmatrix} = \begin{bmatrix} \cos\theta_j & -\sin\theta_j \\ \sin\theta_j & \cos\theta_j \end{bmatrix} \begin{bmatrix} b_{\hat{x}}(\hat{\xi}_j,0) \\ b_{\hat{y}}(\hat{\xi}_j,0) \end{bmatrix} \tag{8}$$

$$\begin{bmatrix} G^{ij}_{\hat{x}\hat{x}\hat{x}}(\hat{x}_i,0;\hat{\xi}_j,0) & G^{ij}_{\hat{y}\hat{x}\hat{x}}(\hat{x}_i,0;\hat{\xi}_j,0) \\ G^{ij}_{\hat{x}\hat{y}\hat{y}}(\hat{x}_i,0;\hat{\xi}_j,0) & G^{ij}_{\hat{y}\hat{y}\hat{y}}(\hat{x}_i,0;\hat{\xi}_j,0) \\ G^{ij}_{\hat{x}\hat{x}\hat{y}}(\hat{x}_i,0;\hat{\xi}_j,0) & G^{ij}_{\hat{y}\hat{x}\hat{y}}(\hat{x}_i,0;\hat{\xi}_j,0) \end{bmatrix}$$

$$= \begin{bmatrix} \cos^2\theta_i & \sin^2\theta_i & \sin 2\theta_i \\ \sin^2\theta_i & \cos^2\theta_i & -\sin 2\theta_i \\ \frac{-\sin 2\theta_i}{2} & \frac{\sin 2\theta_i}{2} & \cos 2\theta_i \end{bmatrix} \begin{bmatrix} G^{ij}_{xxx}(\hat{x}_i,0;\hat{\xi}_j,0) & G^{ij}_{yxx}(\hat{x}_i,0;\hat{\xi}_j,0) \\ G^{ij}_{xyy}(\hat{x}_i,0;\hat{\xi}_j,0) & G^{ij}_{yyy}(\hat{x}_i,0;\hat{\xi}_j,0) \\ G^{ij}_{xxy}(\hat{x}_i,0;\hat{\xi}_j,0) & G^{ij}_{yxy}(\hat{x}_i,0;\hat{\xi}_j,0) \end{bmatrix} \begin{bmatrix} \cos\theta_j & -\sin\theta_j \\ \sin\theta_j & \cos\theta_j \end{bmatrix} \tag{9}$$

where θ_i, θ_j are the crack inclination angle in the global coordinates for the i-th crack branch and the j-th crack branch, respectively.

Now, considering the j-th crack branch to be a distribution of continuous dislocation on the crack line, the induced stresses for $(\hat{x}_i, 0)$ on the i-th crack branch due to the dislocations of crack branch j can be given by

$$\begin{bmatrix} \sigma^{ij}_{\hat{y}\hat{y}}(\hat{x}_i,0) \\ \sigma^{ij}_{\hat{x}\hat{y}}(\hat{x}_i,0) \end{bmatrix} = \frac{2\mu}{\pi(\kappa+1)} \int_{-a_j}^{a_j} \begin{bmatrix} G^{ij}_{\hat{x}\hat{y}\hat{y}}(\hat{x}_i,0;\hat{\xi}_j,0) & G^{ij}_{\hat{y}\hat{y}\hat{y}}(\hat{x}_i,0;\hat{\xi}_i,0) \\ G^{ij}_{\hat{x}\hat{x}\hat{y}}(\hat{x}_i,0;\hat{\xi}_j,0) & G^{ij}_{\hat{y}\hat{x}\hat{y}}(\hat{x}_i,0;\hat{\xi}_j,0) \end{bmatrix} \begin{bmatrix} B_{\hat{x}}(\hat{\xi}_j) \\ B_{\hat{y}}(\hat{\xi}_j) \end{bmatrix} \mathrm{d}\hat{\xi}_i \tag{10}$$

where $B_{\hat{x}}(\hat{\xi}_j) = \mathrm{d}b_{\hat{x}}(\hat{\xi}_j)/\mathrm{d}\hat{\xi}_j$, $B_{\hat{y}}(\hat{\xi}_j) = \mathrm{d}b_{\hat{y}}(\hat{\xi}_j)/\mathrm{d}\hat{\xi}_j$ are the density functions for the distributed dislocations along crack j and a_j is the half crack branch length of crack j.

Considering all the straight cracks, the kinked cracks and the boundary are modeled by dislocations, the induced stresses for $(\hat{x}_i, 0)$ due to all the dislocations can be calculated by the principle of superposition,

$$\begin{bmatrix} \sigma^{i}_{\hat{y}\hat{y}}(\hat{x}_i,0) \\ \sigma^{i}_{\hat{x}\hat{y}}(\hat{x}_i,0) \end{bmatrix} = \frac{2\mu}{\pi(\kappa+1)} \sum_{j=1}^{M} \int_{-a_j}^{a_j} \begin{bmatrix} G^{ij}_{\hat{x}\hat{y}\hat{y}}(\hat{x}_i,0;\hat{\xi}_j,0) & G^{ij}_{\hat{y}\hat{y}\hat{y}}(\hat{x}_i,0;\hat{\xi}_j,0) \\ G^{ij}_{\hat{x}\hat{x}\hat{y}}(\hat{x}_i,0;\hat{\xi}_j,0) & G^{ij}_{\hat{y}\hat{x}\hat{y}}(\hat{x}_i,0;\hat{\xi}_j,0) \end{bmatrix} \begin{bmatrix} B_{\hat{x}}(\hat{\xi}_j) \\ B_{\hat{y}}(\hat{\xi}_j) \end{bmatrix} \mathrm{d}\hat{\xi}_j \tag{11}$$

where $M = m_b + m_s + \sum_{i=1}^{m_k} p_i$ is the total number of crack branches shown in Fig. 1.

Inserting Eq. (11) into Eqs. (3) and (4) for cracks and boundary respectively, we obtain the governing integral equations,

- for cracks:

$$\begin{bmatrix} \sigma^{i}_{\hat{y}\hat{y}}(\hat{x}_i,0) \\ \sigma^{i}_{\hat{x}\hat{y}}(\hat{x}_i,0) \end{bmatrix} = \frac{2\mu}{\pi(\kappa+1)} \sum_{j=1}^{M} \int_{-a_j}^{a_j} \begin{bmatrix} G^{ij}_{\hat{x}\hat{y}\hat{y}}(\hat{x}_i,0;\hat{\xi}_j,0) & G^{ij}_{\hat{y}\hat{y}\hat{y}}(\hat{x}_i,0;\hat{\xi}_j,0) \\ G^{ij}_{\hat{x}\hat{x}\hat{y}}(\hat{x}_i,0;\hat{\xi}_j,0) & G^{ij}_{\hat{y}\hat{x}\hat{y}}(\hat{x}_i,0;\hat{\xi}_j,0) \end{bmatrix} \begin{bmatrix} B_{\hat{x}}(\hat{\xi}_j) \\ B_{\hat{y}}(\hat{\xi}_j) \end{bmatrix} \mathrm{d}\hat{\xi}_j = \begin{bmatrix} 0 \\ 0 \end{bmatrix} \tag{12}$$

for boundary:

$$\begin{bmatrix} \sigma^{i}_{\hat{y}\hat{y}}(\hat{x}_i,0) \\ \sigma^{i}_{\hat{x}\hat{y}}(\hat{x}_i,0) \end{bmatrix} = \frac{2\mu}{\pi(\kappa+1)} \sum_{j=1}^{M} \int_{-a_j}^{a_j} \begin{bmatrix} G^{ij}_{\hat{x}\hat{y}\hat{y}}(\hat{x}_i,0;\hat{\xi}_j,0) & G^{ij}_{\hat{y}\hat{y}\hat{y}}(\hat{x}_i,0;\hat{\xi}_j,0) \\ G^{ij}_{\hat{x}\hat{x}\hat{y}}(\hat{x}_i,0;\hat{\xi}_j,0) & G^{ij}_{\hat{y}\hat{x}\hat{y}}(\hat{x}_i,0;\hat{\xi}_j,0) \end{bmatrix} \begin{bmatrix} B_{\hat{x}}(\hat{\xi}_j) \\ B_{\hat{y}}(\hat{\xi}_j) \end{bmatrix} \mathrm{d}\hat{\xi}_j = \begin{bmatrix} \sigma^{0}_{\hat{2}}(\hat{x}_i,0) \\ \sigma^{0}_{\hat{1}}(\hat{x}_i,0) \end{bmatrix} \tag{13}$$

Now, Eqs. (12) and (13) exactly provide the integral equations for the solution to the problem of a finite plane containing multiple straight and kinked cracks when tractions are applied on the boundary. We need to note that if displacements are given on the boundary, it can also be solved in a similar way, which will not be presented in this paper.

2.4. Numerical solution of integral equations

The Gauss–Chebyshev quadrature method can be used to solve the integral equations (12) and (13) [10,15].

Firstly, we need to transform the integral over the j-th crack branch $[-a_j, a_j]$ to the standard interval $[-1, 1]$ by making the following substitutions:

$$\begin{cases} \hat{\xi}_i = \hat{\xi}_j(\hat{s}_j) = a_j \hat{s}_j \\ \hat{x}_i = \hat{x}_i(\hat{t}_i) = a_i \hat{t}_i \end{cases} \tag{14}$$

Combining Eqs. (14), (12), and (13), we can write:

- for cracks:

$$\begin{aligned} \begin{bmatrix} \sigma^{i}_{\hat{y}\hat{y}}(\hat{x}_i(\hat{t}_i),0) \\ \sigma^{i}_{\hat{x}\hat{y}}(\hat{x}_i(\hat{t}_i),0) \end{bmatrix} &= \frac{2\mu}{\pi(\kappa+1)} \sum_{j=1}^{M} a_j \int_{-a_j}^{a_j} \begin{bmatrix} G^{ij}_{\hat{x}\hat{y}\hat{y}}(\hat{x}_i(\hat{t}_i),0;\hat{\xi}_j(\hat{s}_j),0) & G^{ij}_{\hat{y}\hat{y}\hat{y}}(\hat{x}_i,0;\hat{\xi}_j(\hat{s}_j),0) \\ G^{ij}_{\hat{x}\hat{x}\hat{y}}(\hat{x}_i(\hat{t}_i),0;\hat{\xi}_j,0) & G^{ij}_{\hat{y}\hat{x}\hat{y}}(\hat{x}_i(\hat{t}_i),0;\hat{\xi}_j(\hat{s}_j),0) \end{bmatrix} \begin{bmatrix} B_{\hat{x}}(\hat{\xi}_j(\hat{s}_j)) \\ B_{\hat{y}}(\hat{\xi}_j(\hat{s}_j)) \end{bmatrix} \mathrm{d}\hat{\xi}_j \\ &= \begin{bmatrix} 0 \\ 0 \end{bmatrix} \end{aligned} \tag{15}$$

- for the boundary:

$$\begin{aligned} \begin{bmatrix} \sigma^{i}_{\hat{y}\hat{y}}(\hat{x}_i(\hat{t}_i),0) \\ \sigma^{i}_{\hat{x}\hat{y}}(\hat{x}_i(\hat{t}_i),0) \end{bmatrix} &= \frac{2\mu}{\pi(\kappa+1)} \sum_{j=1}^{M} a_j \int_{-a_j}^{a_j} \begin{bmatrix} G^{ij}_{\hat{x}\hat{y}\hat{y}}(\hat{x}_i(\hat{t}_i),0;\hat{\xi}_j(\hat{s}_j),0) & G^{ij}_{\hat{y}\hat{y}\hat{y}}(\hat{x}_i,0;\hat{\xi}_j(\hat{s}_j),0) \\ G^{ij}_{\hat{x}\hat{x}\hat{y}}(\hat{x}_i(\hat{t}_i),0;\hat{\xi}_j,0) & G^{ij}_{\hat{y}\hat{x}\hat{y}}(\hat{x}_i(\hat{t}_i),0;\hat{\xi}_j(\hat{s}_j),0) \end{bmatrix} \begin{bmatrix} B_{\hat{x}}(\hat{\xi}_j(\hat{s}_j)) \\ B_{\hat{y}}(\hat{\xi}_j(\hat{s}_j)) \end{bmatrix} \mathrm{d}\hat{\xi}_j \\ &= \begin{bmatrix} \sigma^{0}_{\hat{2}}(\hat{x}_i(\hat{t}_i),0) \\ \sigma^{0}_{\hat{1}}(\hat{x}_i(\hat{t}_i),0) \end{bmatrix} \end{aligned} \tag{16}$$

Though multiple kinked cracks are included in this study, however, previous research [10,15] showed that ignoring the exact singularity at the kinks does not make large errors if our primary interest is on the dislocation densities of the crack tips.

So, we can decompose the dislocation density functions for the i-th crack in the following form,

$$\begin{bmatrix} B_{\hat{x}}(\hat{\xi}_i(\hat{s}_i)) \\ B_{\hat{y}}(\hat{\xi}_i(\hat{s}_i)) \end{bmatrix} = \frac{1}{\sqrt{1-\hat{s}_i^2}} \begin{bmatrix} \phi_{\hat{x}}^i(\hat{s}_i) \\ \phi_{\hat{y}}^i(\hat{s}_i) \end{bmatrix} \tag{17}$$

where $\phi_{\hat{x}}^i(\hat{s}_i)$ and $\phi_{\hat{y}}^i(\hat{s}_i)$ are the new unknown functions to be determined and $-1 \le \hat{s}_i \le 1$ is a non-dimensional parameter along i-th crack branch.

Assuming that the i-th crack branch has N integration points and that there are $N-1$ collocation points, the integration and collocation points can be denoted by $\hat{s}_t^i$ $(t = 1, 2, \ldots, N)$ and $\hat{t}_k^i$ $(k = 1, 2, \ldots, N-1)$ respectively:

$$\hat{t}_i = \cos\left(\frac{2i-1}{2N}\pi\right), \qquad \hat{x}_k = \cos\left(\frac{k}{N}\pi\right) \tag{18}$$

For straight cracks in the plane, the condition that there is no-net-dislocation on each embedded crack must be satisfied. So, the following two extra equations are needed to solve the algebraic equations:

$$\begin{aligned} &\sum_{i=1}^{N} \phi_{\hat{x}}^i(\hat{s}_i) = 0 \\ &\sum_{i=1}^{N} \phi_{\hat{y}}^i(\hat{s}_i) = 0 \end{aligned} \tag{19}$$

For each kinked crack, the extra equations can be established based on the connection conditions at the kinks and no-net dislocations for the overall crack [10,15],

$$\begin{aligned} &\sum_{i=1}^{p_i} \left[\frac{a_i \cos\theta_i}{N} \sum_{i=1}^{N} \phi_{\hat{x}}^i(\hat{s}_i) - \frac{a_i \sin\theta_i}{N} \sum_{i=1}^{N} \phi_{\hat{y}}^i(\hat{s}_i) \right] = 0 \\ &\sum_{i=1}^{p_i} \left[\frac{a_i \sin\theta_i}{n_{\mathrm{I}}} \sum_{i=1}^{N} \phi_{\hat{x}}^i(\hat{s}_i) + \frac{a_i \sin\theta_i}{n_{\mathrm{I}}} \sum_{i=1}^{N} \phi_{\hat{y}}^i(\hat{s}_i) \right] = 0 \end{aligned} \tag{20}$$

$$\begin{aligned} &\cos\theta_i \phi_{\hat{x}_i}^i(+1) - \sin\theta_i \phi_{\hat{y}_i}^i(+1) = \cos\theta_{i+1} \phi_{\hat{x}_{i+1}}^{i+1}(+1) - \sin\theta_{i+1} \phi_{\hat{y}_{i+1}}^{i+1}(+1) \\ &\sin\theta_i \phi_{\hat{x}_i}^i(+1) + \cos\theta_i \phi_{\hat{y}_i}^i(+1) = \sin\theta_{i+1} \phi_{\hat{x}_{i+1}}^{i+1}(+1) + \cos\theta_{i+1} \phi_{\hat{y}_{i+1}}^{i+1}(+1) \end{aligned} \tag{21}$$

where p_i is the total number of branches of the kinked crack containing the i-th crack, θ_i is the crack angle of the i-th crack in global coordinates. $\phi(+1), \phi(-1)$ can be determined by [10]

$$\begin{aligned} \phi(+1) &= \sum_{i=1}^{N} \frac{\sin((2i-1)(2N-1)\pi/(4N))}{\sin((2i-1)/(4N))} \phi(s_i) \\ \phi(-1) &= \sum_{i=1}^{N} \frac{\sin((2i-1)(2N-1)\pi/(4N))}{\sin((2i-1)/(4N))} \phi(s_{N+1-i}) \end{aligned} \tag{22}$$

To this end, all the unknown functions $\phi_{\hat{x}}^1(\hat{s}_i)$ and $\phi_{\hat{y}}^1(\hat{s}_i)$ at the end points in the linear algebraic system can be obtained by solving the above equations.

The stress intensity factor of each crack can be readily obtained by the following relationship:

$$\begin{aligned} \left(K_{\mathrm{I}}^-\right)_i &= -\sqrt{\pi a_1} \frac{2\mu}{\kappa+1} \left(\phi_{\hat{y}_1}^1(-1)\right)_i, \qquad \left(K_{\mathrm{II}}^-\right)_i = -\sqrt{\pi a_1} \frac{2\mu}{\kappa+1} \left(\phi_{\hat{x}_1}^1(-1)\right)_i \\ \left(K_{\mathrm{I}}^+\right)_i &= -\sqrt{\pi a_m} \frac{2\mu}{\kappa+1} \left(\phi_{\hat{y}_m}^m(+1)\right)_i, \qquad \left(K_{\mathrm{II}}^+\right)_i = -\sqrt{\pi a_m} \frac{2\mu}{\kappa+1} \left(\phi_{\hat{x}_m}^m(+1)\right)_i \end{aligned} \tag{23}$$

where, for a kinked crack, $(K_{\mathrm{I}}^-)_i$, $(K_{\mathrm{II}}^-)_i$ represent the mode-I and mode-II stress intensity factors of the left crack tip of crack branch 1 for the i-th kinked crack, and a_1 is the half crack length of the first crack branch for the i-th kinked crack. Similarly, $(K_{\mathrm{I}}{}^+)_i$, $(K_{\mathrm{II}}{}^+)_i$ represent the mode-I and mode-II stress intensity factors of the right crack tip of crack branch m for the i-th kinked crack, and a_m is the half crack length of the last crack branch for the i-th kinked crack. For a straight crack, $(K_{\mathrm{I}}^-)_i$, $(K_{\mathrm{II}}^-)_i$ represent the mode-I and mode-II stress intensity factors of the left crack tip, and $(K_{\mathrm{I}}^+)_i$, $(K_{\mathrm{II}}^+)_i$ represent the mode-I and mode-II stress intensity factors of the right crack tip. a_1 is the half crack length of crack i.

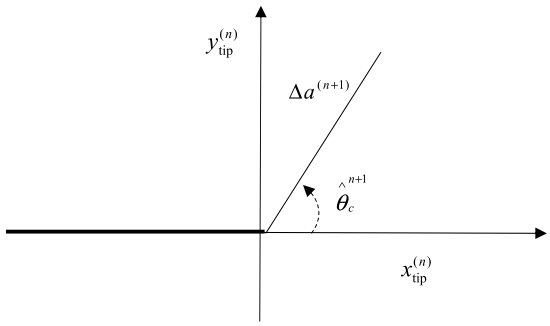

Fig. 4. Crack propagation in the local coordinate system of the crack for the $n+1$th step.

3. Fatigue crack growth analysis

Fatigue crack propagation can be realized by a number of incremental steps extending the crack tips to a new position based on Paris's equation,

$$\frac{\mathrm{d}a}{\mathrm{d}N} = C(\Delta K_{\mathrm{I\,eq}})^m \tag{24}$$

where C and m are the material constants, a is the crack length, N is the number of loading cycles. $\Delta K_{\mathrm{I\,eq}}$ can be calculated by the following equation with ΔK_{I} and ΔK_{II} instead of K_{I} and ΔK_{II}.

$$K_{\mathrm{I\,eq}} = K_{\mathrm{I}}\cos^3\frac{\theta_c}{2} - 3K_{\mathrm{II}}\cos^2\frac{\theta_c}{2}\sin\frac{\theta_c}{2} \tag{25}$$

The complexity of the simulation of the propagation of multiple cracks is that all the cracks simultaneously have different growth increments Δa_i and different crack turning angles $\hat{\theta}_c^i$ for crack tip i.

The maximum circumferential stress criterion is selected to determine the crack propagation turning angle $\hat{\theta}_c$ as shown in Fig. 4:

$$\hat{\theta}_c = 2\arctan\frac{-2K_{\mathrm{II}}}{K_{\mathrm{I}} + \sqrt{K_{\mathrm{I}}^2 + 8K_{\mathrm{II}}^2}} \tag{26}$$

In Fig. 4, x_{tip}^n, y_{tip}^n represent the location of the crack tip in the local coordinate system of the crack, respectively, after n-step propagation. $\Delta a^{(n+1)}$, $\hat{\theta}_c^{n+1}$ represent the crack propagation length and the crack propagation turning angle for the $n+1$th step.

The crack propagation length of each crack tip can be calculated by the following equation for multiple cracks:

$$\Delta a_i = \Delta a_{\max}\left(\frac{\Delta K_{\mathrm{I\,eq}}^i}{\Delta K_{\mathrm{I\,eq,max}}^i}\right)^m \tag{27}$$

where Δa_i is the propagation length of the i-th crack tip. $\Delta a_{\max}$ is the maximum value of the crack propagation length corresponding to the crack tip with the largest $\Delta K_{\mathrm{I\,eq}}$. The maximum crack propagation length is fixed in this study.

Once the crack growth increment and the turning angle for every crack tip are obtained, we can readily extend the crack tip to a new position by the following equation,

$$\begin{aligned} \theta^{(n+1)} &= \theta^{(n)} + \hat{\theta}_c^{(n)} \\ x_{\text{tip}}^{(n+1)} &= x_{\text{tip}}^{(n)} + \Delta a\left(\cos\left(\theta^{(n+1)}\right)\cdot\sin\left(\theta^{(n+1)}\right)\right) \end{aligned} \tag{28}$$

Then a new model containing multiple cracks is obtained. By modeling the new cracks by a series of distributed dislocations, the stress intensity factors of the new cracks will be obtained. In this end, fatigue propagation of multiple cracks can be realized by repeating the whole process.

4. Numerical examples

In this section, numerical examples for calculating the intensity factors of multiple cracks in a finite plane will be presented first. Then examples of the simulation of the propagation of multiple cracks in a finite plane will be given. All the calculations are carried out using a personal computer with 2.0 GHz and i5 CPU and in all examples, plane strain conditions are assumed.

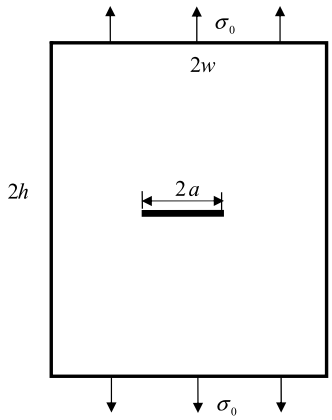

Fig. 5. A rectangular plate containing a central straight crack.

Table 1
Normalized stress intensity factor for a central crack in a finite plane.

a/w	h/w	F_I (presented method) $N = 5$	F_I (presented method) $N = 10$	F_I (presented method) $N = 15$	F_I (presented method) $N = 20$	F_I (reference [22])	F_I (reference [23])
0.1	0.35	1.0208	1.1007	1.0888	1.0895	1.0895	1.0881
0.1	0.5	1.0263	1.0465	1.0457	1.0457	1.0457	1.0450
0.1	0.75	1.0202	1.0232	1.0232	1.0232	1.0233	1.0227
0.1	1.0	1.0129	1.0139	1.0139	1.0139	1.0139	1.0136
0.1	1.25	1.0083	1.0091	1.0091	1.0091	1.0092	1.0090
0.1	2	1.0045	1.0062	1.0061	1.0061		1.0060
0.3	0.35	1.2378	1.6213	1.6401	1.6407	1.6407	1.6325
0.3	0.5	1.2612	1.3690	1.3706	1.3707	1.3709	1.3654
0.3	0.75	1.1838	1.2038	1.2043	1.2045	1.2047	1.1995
0.3	1.0	1.1139	1.1227	1.1230	1.1231	1.1232	1.1198
0.3	1.25	1.0735	1.0825	1.0826	1.0827	1.0827	1.0816
0.3	2	1.0424	1.0606	1.0580	1.0583		1.0580
0.5	0.35	2.5865	2.4825	2.4628	2.4634	2.4639	2.4441
0.5	0.5	1.9239	1.9636	1.9649	1.9658	1.9671	1.9463
0.5	0.75	1.5145	1.5505	1.5524	1.5534	1.5537	1.5366
0.5	1.0	1.2998	1.3329	1.3333	1.3335	1.3337	1.3255
0.5	1.25	1.1983	1.2397	1.2381	1.2384	1.2383	1.2358
0.5	2	1.1376	1.2058	1.1839	1.1883		1.1865
0.7	0.35	6.2538	4.0626	4.0168	4.0226	4.0313	3.9407
0.7	0.5	3.1044	3.0194	3.0297	3.0340	3.0395	2.9547
0.7	0.75	1.9366	2.0529	2.0518	2.0529	2.0534	2.0202
0.7	1.0	1.5414	1.6927	1.6749	1.6778	1.6771	1.6654
0.7	1.25	1.4104	1.5847	1.5403	1.5497	1.5480	1.5431
0.7	2	1.3942	1.5933	1.4398	1.4890		1.4848
0.8	0.35		5.7187	5.6645	5.7023	5.7085	5.4528
0.8	0.5	3.7968	3.7568	3.7604	3.7712	3.7726	3.6316
0.8	0.75	2.1160	2.4370	2.3820	2.3922	2.3897	2.3542
0.8	1.0	1.7325	2.0910	1.9638	1.9913	1.9908	1.9773
0.8	1.25	1.6465	2.0140	1.8105	1.8688	1.8677	1.8595
0.8	2	1.7233	1.9960	1.6618	1.8171		1.8068

Example 1. A rectangular plate containing a central straight crack.

A rectangular plate of height $2h$ and width $2w$ containing a central straight crack of length $2a$ is subjected to a uniform tensile stress σ_0 at its top and bottom edges, as shown in Fig. 5. The computed normalized stress intensity factor of the crack tip is defined as

$$F_I = K_I/\sigma_0\sqrt{\pi a}$$

In this example, the ratio a/w is set at 0.1, 0.3, 0.5, 0.7, and 0.8, h/w is chosen as 0.35, 0.5, 0.75, 1.0, 1.25, and 2.0. Meanwhile, the numbers of integration points N are set at 5, 10, 15, and 20. The values of F_I for different values of a/w, h/w, and N are shown in Table 1. For comparison purposes, Table 1 also lists the numerical results reported in Refs. [23] and [24].

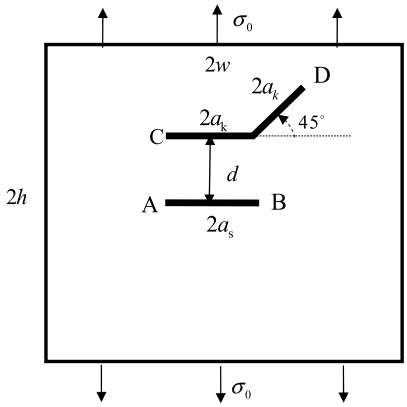

Fig. 6. A rectangular plate containing a straight crack and a kinked crack.

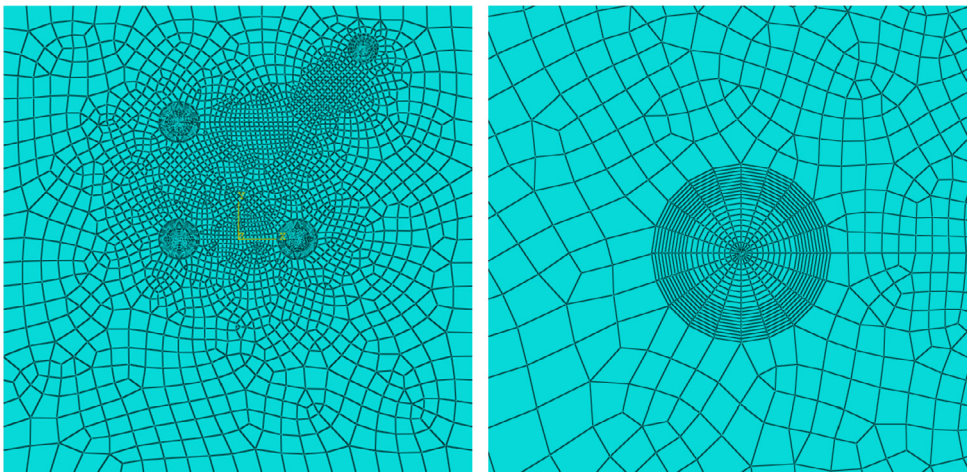

(a) (b)

Fig. 7. The finite element model: (a) mesh for the whole model; (b) the mesh near the crack tip.

As we can see from Table 1, the results obtained by the present method become more accurate when increasing the number of integration points. The results obtained by the presented method agree very well with the previous research and yield a very high accuracy when the number of integration points is 20. So, if not specified otherwise, the number of integration points is fixed at 20 in the following study.

Example 2. A rectangular plate containing a straight crack and a kinked crack.

A rectangular plate of height $2h$ and width $2w$ containing a straight crack of length $2a_s$ and a kinked crack is subjected to a uniform tensile stress σ_0 at its top and bottom edges. The kinked crack has two branches of length $2a_k$ and the kinked branch makes an angle of 45° with the main crack, as shown in Fig. 6. In order to validate the present method for this problem, finite element analysis was used to study the same problem and the detailed mesh model in the finite element analysis is shown in Fig. 7.

In this example, the following geometric parameters are selected:

$$2b = 2h = 80 \text{ mm}, \qquad 2a_k = 10 \text{ mm}, \qquad d = 20 \text{ mm}$$

The calculated normalized stress intensity factors of the crack tips A, B, C, D are defined as

$$F_{\mathrm{I(A)}} = K_{\mathrm{I(A)}}/\sigma\sqrt{\pi a_s}, \qquad F_{\mathrm{I(B)}} = K_{\mathrm{I(B)}}/\sigma\sqrt{\pi a_s}, \qquad F_{\mathrm{I(C)}} = K_{\mathrm{I(C)}}/\sigma\sqrt{\pi(2a_k)}$$
$$F_{\mathrm{I(D)}} = K_{\mathrm{I(D)}}/\sigma\sqrt{\pi(2a_k)}, \qquad F_{\mathrm{II(D)}} = K_{\mathrm{II(D)}}/\sigma\sqrt{\pi(2a_k)}$$

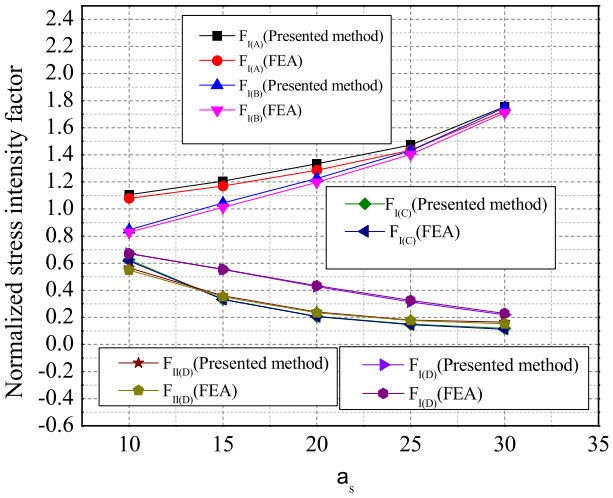

Fig. 8. Variation of the normalized stress intensity factor for a straight crack and a kinked crack in a plate.

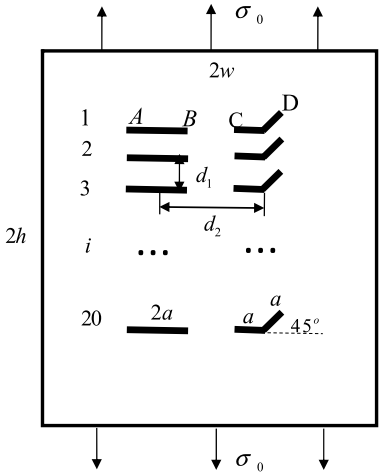

Fig. 9. A rectangular plate containing multiple straight cracks and kinked cracks.

In the calculation, we chose the length of the straight crack $2a_s$ to be 10 mm, 20 mm, 30 mm, 40 mm, 50 mm, 60 mm. The variation of $F_{\mathrm{I(A)}}$, $F_{\mathrm{I(B)}}$, $F_{\mathrm{I(C)}}$, $F_{\mathrm{I(D)}}$, $F_{\mathrm{II(D)}}$ are shown in Fig. 8.

As we can see from Fig. 8, the results obtained by the presented method and those of the FEA method are in very good agreement. The maximum error between them is 6.47% for $F_{\mathrm{II(D)}}$ when $2a_s = 60$ mm. This is because the straight crack is very long and $F_{\mathrm{II(D)}}$ is very small (about 0.15). All the other errors between these two methods are less than 2%. This problem can only be solved in about 0.9 s only by the presented method; however, the finite element method would take about 30 s. We can see that the solution is accurate enough and efficient if the number of integration points used for the cracks is 20.

In this example, there are only one straight crack and one kinked crack. However, the presented method is capable of solving the problem for any number of straight cracks and kinked cracks.

Example 3. A rectangular plate containing 20 straight cracks and 20 kinked cracks.

A rectangular plate (height $2h$, width $2w$) containing 20 straight cracks and 20 kinked cracks is subjected to a uniaxial loading. The geometry and arrangement of these cracks are shown in Fig. 9. All the straight cracks have the same length $2a$. All the kinked cracks have the same inclination angle of 45° and length a. They are equally spaced in the plane with distances d_1 and d_2.

In the simulation, the following geometric parameters are selected:

$$2w = 2h = 100\ \mathrm{mm}, \qquad d_1 = 5\ \mathrm{mm}, \qquad d_2 = 20\ \mathrm{mm}, \qquad a = 5\ \mathrm{mm}$$

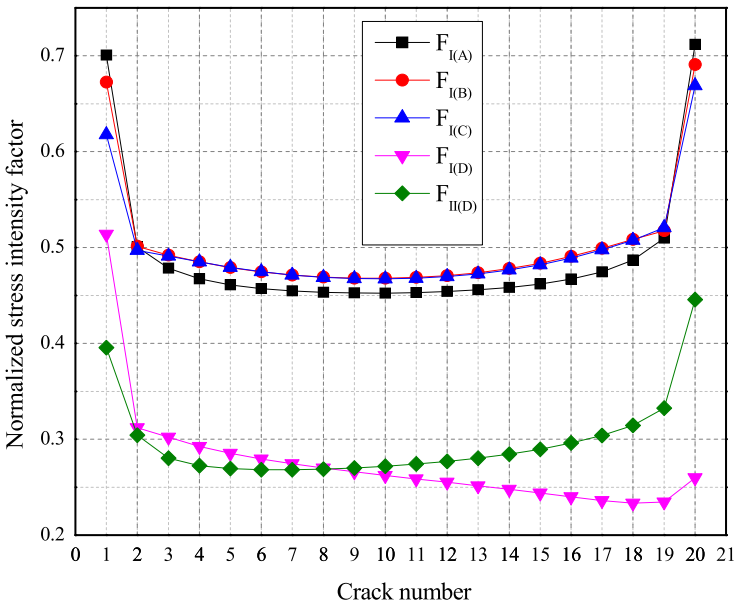

Fig. 10. Stress intensity factor for 20 straight cracks and 20 kinked cracks.

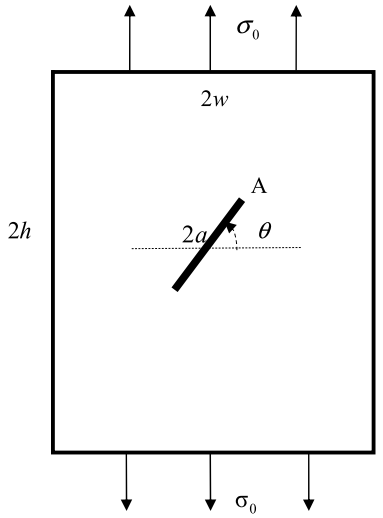

Fig. 11. A plate containing a central inclined crack.

Here we need to mention that all the straight cracks have their own crack tips A and B. Similarly, all the kinked cracks have their own crack tip C and D. The normalized stress intensity factors of the crack tip A, B, C, D are defined as

$$F_{\mathrm{I(A)}} = K_{\mathrm{I(A)}}/\sigma\sqrt{\pi a} \qquad F_{\mathrm{I(B)}} = K_{\mathrm{I(B)}}/\sigma\sqrt{\pi a} \qquad F_{\mathrm{I(C)}} = K_{\mathrm{I(C)}}/\sigma\sqrt{\pi a}$$
$$F_{\mathrm{I(D)}} = K_{\mathrm{I(D)}}/\sigma\sqrt{\pi a} \qquad F_{\mathrm{II(D)}} = K_{\mathrm{II(D)}}/\sigma\sqrt{\pi a}$$

The normalized stress intensity factors of all the cracks are shown in Fig. 10.

As we can see from Fig. 10, the outside cracks (crack number 1 and number 20) usually have higher normalized stress intensity factors than the inner cracks. The normalized stress intensity factors almost distribute symmetrically along crack number 10 and number 11. In this example, there are totally 64 cracks in total and the computation time is about 3 min when the number of integration points used for both cracks and boundary is 20.

Example 4. Fatigue crack growth for a rectangular plate containing a central crack.

A rectangular plate ($2h = 2w = 50$ mm) containing a central crack with a length $2a = 10$ mm and an inclination angle θ is subjected to a cyclic stress ($\sigma_0^{\max} = 1$ MPa, $\sigma_0^{\min} = 0$ MPa) perpendicular to the boundaries, as shown in Fig. 11. The

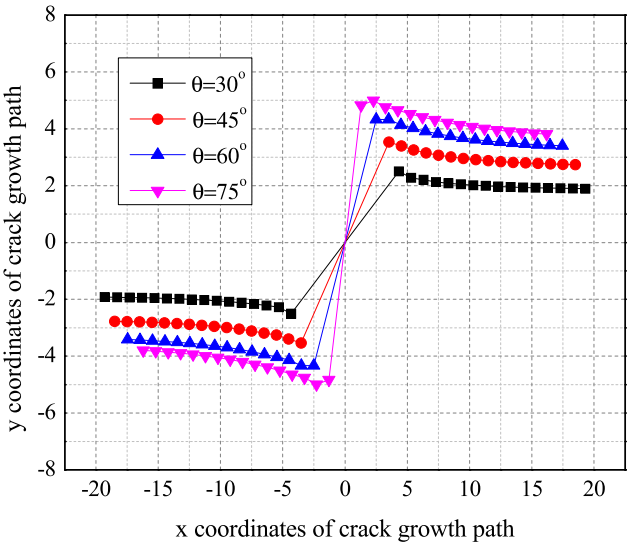

Fig. 12. Crack propagation path of the plate with a central inclined crack.

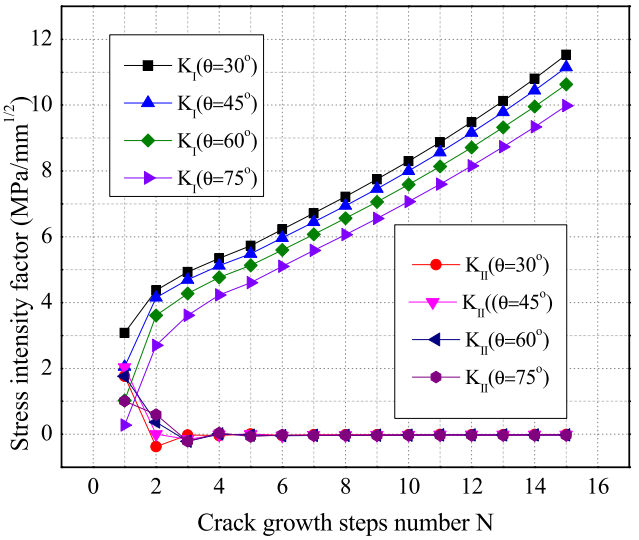

Fig. 13. Stress intensity factor for a central inclined crack with different inclination angles in a plate.

maximum crack increment $\Delta a_{\max}$ is set at 1 mm in this simulation. θ is set at 30°, 45°, 60°, and 75°. The crack growth paths and stress intensity factors at crack tip A are shown in Fig. 12 and Fig. 13, respectively.

The results obtained by the presented method agree very well with those of reference [25].

Example 5. A rectangular plate containing two non-collinear cracks.

For a comparison purpose with reference [25], considering a rectangular plate ($2h = 180$ mm, $2w = 90$ mm) containing two parallel non-collinear and non-angled cracks with a length $2a = 10$ mm is subjected to a cyclic stress ($\sigma_0^{\max} = 160$ MPa, $\sigma_0^{\min} = 0$ MPa) perpendicular to the boundaries, as shown in Fig. 14. The horizontal and vertical distances between the tips of the two central cracks are $d_1 = 5$ mm and $d_2 = 15$ mm, respectively.

The maximum crack increment $\Delta a_{\max}$ is set at 2 mm in this simulation. The crack growth paths of the two non-collinear cracks are shown in Fig. 15. The stress intensity factors of the crack tips A and B are shown in Fig. 16, respectively. Both the fatigue growth paths and the stress intensity factor are in very good agreement with reference [25].

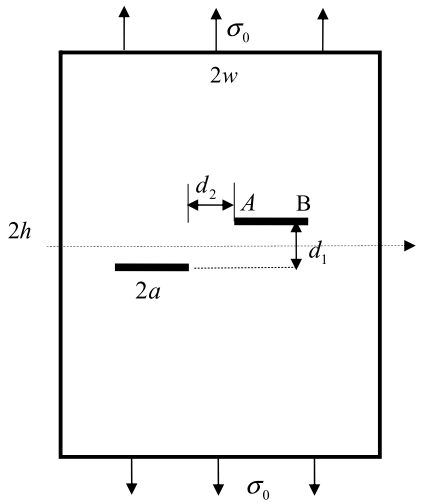

Fig. 14. A rectangle plate containing two non-collinear cracks.

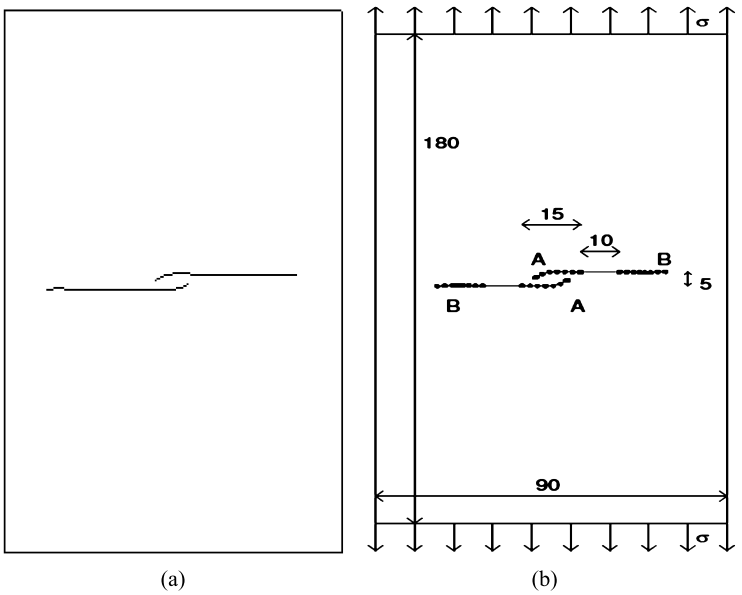

Fig. 15. Fatigue growth paths for two non-collinear cracks in a plane: (a) as predicted by present method, (b) as predicted by reference [24].

Example 6. A rectangular plate containing two crossed cracks.

A rectangular plate ($2h = 180$ mm, $2w = 90$ mm) containing two crossed cracks with a length $2a = 10$ mm located at the center of the plate is subjected to a cyclic stress as shown in Fig. 17. The two cracks have inclination angles of θ and $\pi - \theta$, respectively. The crack growth paths of the two crossed cracks are shown in Fig. 18. As we can see here, the presented method is an effective way to simulate complicated crack problems.

Example 7. A rectangular plate containing six parallel cracks.

A rectangular plate ($2h = 180$ mm, $2w = 90$ mm) containing six parallel cracks in two rows with a length $2a = 10$ mm is subjected to a cyclic stress as shown in Fig. 19. The vertical distance between the two rows is $d_1 = 5$ mm. The horizontal distance between the inner crack tips is $d_1 = 15$ mm. The crack growth paths of these six cracks are shown in Fig. 20.

Though here only six cracks are included in this plate, this method can simulate the growth of any number of arbitrary fatigue cracks with an inclination angle. This will not be presented here.

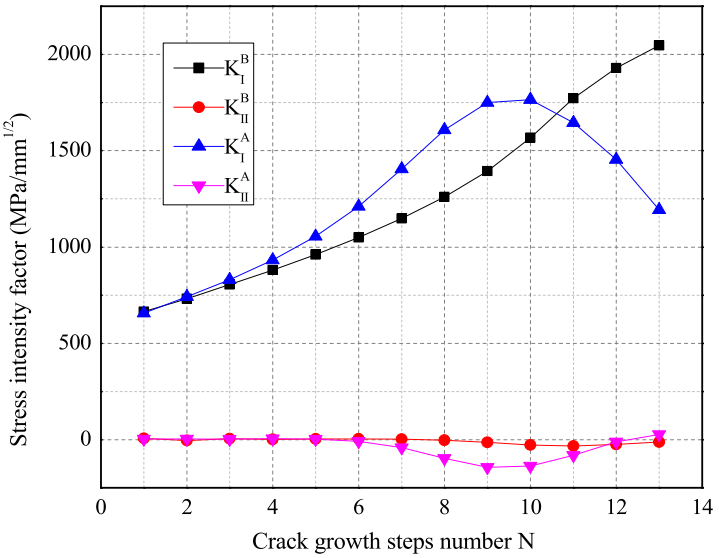

Fig. 16. Stress intensity factor for two non-collinear cracks in a finite plane.

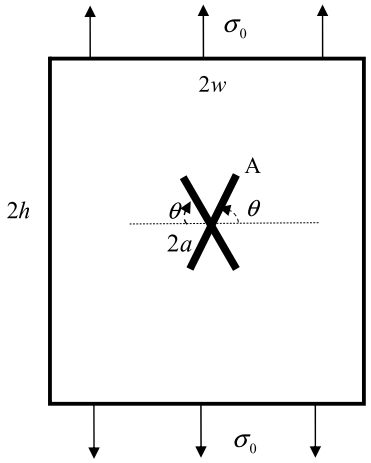

Fig. 17. A rectangle plate containing two crossed cracks.

5. Conclusion

In this paper, an automated numerical study of multiple cracks propagation in a finite plane is presented. Firstly, a solution for a two-dimensional finite elastic plane containing multiple straight and kinked cracks is presented. All the cracks and boundaries are modeled by the distributed dislocations in an infinite plane. The mixed-mode stress intensity factors of all the cracks can be obtained. Then the maximum circumferential stress criterion is used to calculate the crack turning angle of each crack tip. The well-known Paris law is adopted to calculate the growth length for each crack tip at each step. Several numerical examples illustrate that the presented method is very convenient to model multiple cracks in a 2D finite plane and is very effective in simulating the propagation of multiple cracks.

Acknowledgements

This work was financially supported by the National Natural Science Foundation of China (Nos. 51674200, 20873999, 51802229, and 51605140), the Natural Science Foundation of Guangdong Province (Nos. 2018A030313430 and 2018A 030313561), and the Innovation and Strong School Engineering Foundation of Guangdong Province (Nos. 2017KQNCX201, 2016KQNCX169, and 2017KQNCX197).

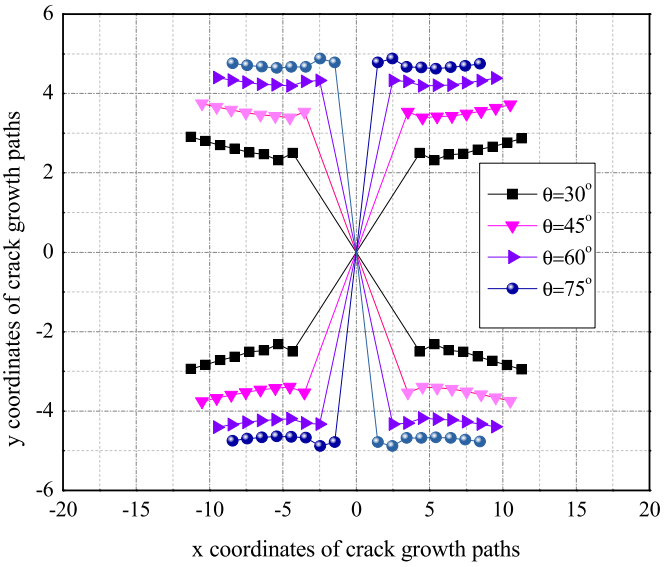

Fig. 18. Fatigue crack growth paths for two crossed cracks in a finite plane.

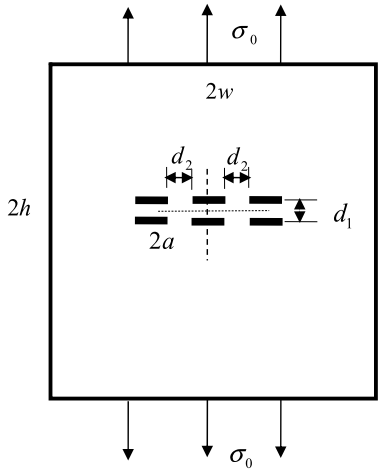

Fig. 19. A rectangular plate containing six parallel cracks.

Fig. 20. Fatigue crack growth paths for six parallel cracks in a finite plane.

References

[1] P.O. Bouchard, F. Bay, Y. Chastel, Numerical modeling of crack propagation: automatic remeshing and comparison of different criteria, Comput. Methods Appl. Mech. Eng. 192 (2003) 3887–3908.
[2] H. Chi, C. Talischi, O. Lopez-Pamies, G.H. Paulino, Polygonal finite elements for finite elasticity, Int. J. Numer. Methods Eng. 101 (2015) 305–328.
[3] A.R. Khoei, R. Yasbolaghi, S.O.R. Biabanaki, A polygonal finite element method for modeling crack propagation with minimum remeshing, Int. J. Fract. 194 (2015) 123–148.
[4] Z. Wang, L. Ma, L. Wu, Numerical simulation of crack growth in brittle matrix of particle reinforced composites using the XFEM technique, Acta Mech. Solida Sin. 25 (2012) 9–21.
[5] S. Natarajan, P. Kerfriden, D. Roy Mahapatra, Numerical analysis of the inclusion–crack interaction by the extended finite element method, Int. J. Comput. Methods Eng. Sci. Mech. 15 (2014) 26–32.
[6] F. Erdogan, G.D. Gupta, M. Ratwani, Interaction between a circular inclusion and an arbitrarily oriented crack, J. Appl. Mech. 41 (1974) 1007–1013.
[7] M. Comninou, F.-K. Chang, Effects of partial closure and friction on a radial crack emanating from a circular hole, Int. J. Fract. 28 (1985) 29–36.
[8] D.A. Hills, M. Comninou, A normally loaded half plane with an edge crack, Int. J. Solids Struct. 21 (1985) 399–410.
[9] D. Nowell, D.A. Hills, Open cracks at or near free of positive radial stresses along the crack line in the edges, J. Strain Anal. Eng. Des. 22 (1987) 177–185.
[10] D.A. Hills, P.A. Kelly, D.N. Dai, A.M. Korsunsky, Solution of Crack Problems – the Distributed Dislocation, Kluwer Academic Publishers, Dordrecht, 1996.
[11] J. Weertman, Dislocation Based Fracture Mechanics, World Scientific, Singapore, 1996.

[12] X. Li, X. Jiang, X. Li, Solution of an inclined crack in a finite plane and a new criterion to predict fatigue crack propagation, Int. J. Mech. Sci. 119 (2016) 217–223.
[13] L. Xiaotao, L. Xu, J. Xiaoyu, Influence of a micro-crack on the finite macro-crack, Eng. Fract. Mech. 177 (2017) 95–103.
[14] X. Jin, L. Keer, Solution of multiple edge cracks in an elastic plane, Int. J. Fract. 137 (2006) 121–137.
[15] X. Jin, Analysis of Some Two-Dimensional Problems Containing Cracks and Holes, Northwestern University, Evanston, USA, 2006.
[16] N. Hallback, M.W. Tofique, Development of a distributed dislocation dipole technique for the analysis of multiple straight, kinked and branched cracks in an elastic half-plane, Int. J. Solids Struct. 51 (2014) 2878–2892.
[17] D.N. Dai, Modeling cracks in finite bodies by distributed dislocation dipoles, Fatigue Fract. Eng. Mater. Struct. 25 (2002) 27–39.
[18] J.J. Han, M.D. Hanasekar, Modelling cracks in arbitrarily shaped finite bodies by distribution of dislocation, Int. J. Solids Struct. 41 (2004) 399–411.
[19] J. Zhang, Z. Qu, Q. Huang, Solution of multiple cracks in a finite plate of an elastic isotropic material with the distributed dislocation method, Acta Mech. Solida Sin. 27 (2014) 276–283.
[20] K. Sharma, S. Singh, Numerical distributed dislocation modeling of multiple cracks in piezoelectric media considering different crack-face boundary conditions and finite size effects, Strength Fract. Complex. 10 (2017) 49–72.
[21] K. Sharma, T.Q. Bui, R.R. Bhargava, Numerical studies of an array of equidistant semi-permeable inclined cracks in 2-D piezoelectric strip using distributed dislocation method, Int. J. Solids Struct. 80 (2016) 137–145.
[22] F. Erdogan, G.D. Gupta, T.S. Cook, Numerical solution of singular integral equations, in: G.C. Sih (Ed.), Methods of Analysis and Solutions of Crack Problems, Noordhoff, Leyden, The Netherlands, 1973.
[23] Y.Z. Chen, Z.X. Wang, Solution of multiple crack problems in a finite plate using coupled integral equations, Int. J. Solids Struct. 49 (2012) 87–94.
[24] Y.Z. Chen, X.Y. Lin, Z.X. Wang, Evaluation of the T-stress and stress intensity factor for a cracked plate in general case using eigenfunction expansion variational method, Fatigue Fract. Eng. Mater. Struct. 31 (2008) 476–487.
[25] M. Duflot, H. Nguyen-Dang, A meshless method with enriched weight functions for fatigue crack growth, Int. J. Numer. Methods 59 (2004) 1945–1961.